The Korean Journal of Ceramics, **3** [2] 116 - 123 (1997)

Characterization of Chemically Stabilized β-cristobalite Synthesized by Solution-Polymerization Route

Sang-Jin Lee

Department of Materials Science and Engineering, University of Illinois at Urbana-Champaign, Urbana, Illinois 61801, USA

(Received May 15, 1997)

A chemically stabilized β-cristobalite, which is stabilized by stuffing cations of Ca^{2+} and Al^{3+}, was prepared by a solution-polymerization route employing Pechini resin or PVA solution as a polymeric carrier. The polymeric carrier affected the crystallization temperature, morphology of calcined powder, and particle size distribution. In case of the polyvinyl alcohol (PVA) solution process, a fine β-cristobalite powder with a narrow particle size distribution (average particle size: 0.3 μm) and a BET specific surface area of 72 m^2/g was prepared by an attrition-milling for 1 h after calcination at 1100°C for 1 h. Wider particle size distribution and higher specific surface area were observed for the β-cristobalite powder derived from Pechini resin. The cubic(β)-to-tetragonal(α) phase transformation in polycrystalline β-cristobalite was induced at approximately 180°C. Like other materials showing transformation toughening, a critical size effect controlled the β-to-α transformation. Densified cristobalite sample had some cracks in its internal texture after annealing. The cracks, occurred spontaneously on cooling, were observed in the sample with an average grain sizes of 4.0 μm or above. In case of the sintered cristobalite having a composition of $CaO \cdot 2Al_2O_3 \cdot 40SiO_2$, small amount of amorphous phase and slow grain growth during annealing were observed. Shear stress-induced transformation was also observed in ground specimen. Cristobalite having a composition of $CaO \cdot 2Al_2O_3 \cdot 80SiO_2$ showed a more sensitive response to shear stress than the $CaO \cdot 2Al_2O_3 \cdot 40SiO_2$ type cristobalite. Shear-induced transformation resulted in an increase of volume about 13% in α-cristobalite phase on annealing for above 10 h in the case of the former composition.

Key words : β-cristobalite, Solution-polymerization route, Critical size effect, Transformation

I. Introduction

β-cristobalite, a high-temperature polymorphic form of SiO_2, has SiO_4 tetrahedra arranged in a diamond-like lattice with shared corners.[1] On cooling, the fully expanded structure undergoes a reversible displacive phase transformation to a collapsed α-form at about 265°C. This transformation involves a volume decrease of approximately 3.2%.[2,3] The materials, which show a displacive or martensitic phase transformation with a negative volume change or unit cell shape change, are suitable for exploiting the "phase transformation weakening" mechanism. The "phase transformation weakening" mechanism has been demonstrated in several materials by Kriven.[4-6] In phase transformation weakening phenomenon, the crack energy was consumed both in the nucleation of the phase transformation and in the creation of new surfaces in the transformation weakening interphase.[6-8]

The temperature of the α-β inversion in cristobalite is variable and depends on the crystal structure of the starting material.[3,9] In order to obtain the β-cristobalite phase at room temperature, β-cristobalite structure can be chemically stabilized with "stuffing" cations.[10,11] Especially, in the CaO-Al_2O_3-SiO_2 system, the incorporation of foreign ions (Ca^{2+}) in the interstices of silicate structures is charge compensated by the substitution of Al^{3+} for Si^{4+} in the framework.[12-14] The presence of foreign ions in the interstices presumably inhibits the contraction of the structure, which would normally occur during the α-β cristobalite transition. Thus, the chemically stabilized cristobalite containing CaO and Al_2O_3 as dopants, has characteristics of the cubic β form at room temperature rather than the tetragonal α form.

In this work, the preparation of a fine and homogeneous β-cristobalite powder by a solution-polymerization route[15-18] is discussed. The solution-polymerization route, better known as "Pechini type" process,[19,20] was suggested to produce a stable and atomistically homogeneous powder without using expensive and unstable alkoxides. Furthermore, this process is a simple and low-cost process. In the Pechini type process, the Pechini resin[21,22] was used as an organic carrier of pre-ceramic powders.[23] The Pechini resin consisted of citric acid as a chelating agent and ethylene glycol as a polymerizing agent for esterification process. In this work, a rather simple-structured and inexpensive polymer, polyvinyl alcohol(PVA), is also used in the solution-polymerization route. The PVA polymer which is a non-chelating polymer having large chain molecules as the polymeric carrier has hydroxyl functional groups.[15,24] A

stearic entrapment of the metal ions is achieved by using these large chain molecules.[15,17] Both cases are suggested to form a soft and bulky precursor.[15,17,20]

The aim of this study is to prepare a fine and pure β-cristobalite powder by the solution-polymerization route and to find out the effect of dopant content and heat treatment on induced phase transformation behavior of the chemically stabilized β-cristobalite.

II. Experimental Procedure

1. Preparation of chemically stabilized β-cristobalite

The chemically stabilized β-cristobalite with a composition of CaO-Al_2O_3-SiO_2 was synthesized with two kinds of polymeric carriers, Pechini resin or PVA solution, by the solution-polymerization method. A clear sol was prepared from Ludox SK Colloidal silica (25 wt% suspension in water, Du Pont Chemicals, Wilmington, DE) as a source of silica, aluminum nitrate nonahydrate ($Al(NO_3)_3 \cdot 9H_2O$, reagent grade, Aldrich Chemical Co., Milwaukee, WI), and calcium nitrate hexahydrate ($Ca(NO_3)_2 \cdot 4H_2O$, reagent grade, Aldrich Chemical Co., Milwaukee, WI) in proportions to achieve various final compositions. After mixing these reagents with DI water, the polymeric carrier was added, and then the mixture was heated up to 120°C.

Either the Pechini resin or the PVA solution as the polymeric carriers was added to the mixture. The 85 wt% Pechini resin,[22] which consisted of 50 mol% citric acid monohydrate and 50 mol% ethylene glycol, was used in this process. The PVA solution was made from 5 wt% PVA (degree of polymerization-1700) dissolved in water. The amount of the PVA to cation sources in the solution were adjusted in such a way that there were 4 times more positively charged valences of cations than the negatively charged functional ends of the organics.[15] As viscosity of the solution increased by evaporation of water, the mixture was vigorously stirred. The remaining water was then dried, transforming the gel into a porous solid.

Finally, the precursors were crushed and calcined at 1100°C for 1 h. The heating rate was 10°C/min. To produce finer particles, the calcined powder was subjected to attrition milling at 180 rpm for 1 h. The charge included 30 g calcined powder with 1 kg zirconia ball media (ball diameter: 5 mm). The jar volume was 1200 ml and 500 ml iso-propyl alcohol was used as a medium for milling. The attrition milled and dried powder was uniaxially pressed at 20 MPa followed by iso-static pressing at 170 MPa for 10 min. The pellet-shaped green compacts were sintered at 1300°C for 1 h, and finally cooled down to room temperature at furnace cooling rate. After sintering, each sample was subjected to annealing at 1250°C for various times. The stress-induced transformation was achieved by grinding the annealed specimens on a 800 mesh SiC paper.

2. Characterization

(A) Thermal Analysis: The pyrolysis and decomposition behavior of crushed precursors were monitored by simultaneous differential scanning calorimetry and thermogravimetric analysis (DSC/TGA) (Model STA 409, Netzsch GmbH, Selb, Germany) up to 1200°C at a heating rate of 5°C/min, in an air atmosphere.

(B) Specific Surface Area Measurement: The specific surface area of the calcined powders and attriton-milled powders were measured by nitrogen gas absorption (Model ASAP 2400, Micromeritics, Norcross, GA). The surface area data were obtained by five-point BET analysis.

(C) Average Grain Size Measurement: The average grain size of the sintered cristobalite after annealing was analyzed according to the Jeffries-Saltykov method.[25]

(D) Porosity Measurement: The porosity of the sintered body at different sintering temperature was measured by Archimedeswater displacement technique.

(E) X-ray Diffraction Analysis: The phase change between α and β-cristobalite was studied as a function of heating temperature and annealing time using a Rigaku spectrometer (DMax automated powder diffractometer, Rigaku/USA, Danvers, MA) with CuKα radiation (40 kV, 40 mA). The relative ratio of α and β-cristobalite phases were determined by integrating the X-ray peak areas of (102) of α-cristobalite and (222) of β-cristobalite by the equation:[26]

$$V_\alpha = I(102)_\alpha / I(222)_\beta + I(102)_\alpha$$

in which, V_α was the volume fraction of α-cristobalite, and $I(102)_\alpha$ and $I(222)_\beta$ were the peak intensities of $(102)_\alpha$ and $(222)_\beta$, respectively.

(F) Thermal Expansion Behavior: The thermal expansion behavior of sintered polycrystalline cristobalite samples was determined with a recording dilatometer (Netzsch Dilatometer, 402E, Germany) up to 1100°C at a heating rate of 5°C/min.

(G) Electron Microscopy: The powder morphology and microstructure of sintered cristobalite were examined by scanning electron microscopy, (SEM, ISI DS-130, International Scientific Instruments, Santa Clara, CA). To observe grain size and microcracks, polished and then annealed samples were chemically etched in boiling phosphoric acid for 30 sec. The grain morphology and selected area diffraction patterns were examined by transmission electron microscopy, (TEM, Philips EM-420, Philips instruments, Inc., Mahwah, NJ). The TEM specimens were prepared by standard ceramic polishing, dimpling and ion-milling techniques.

III. Results

1. Effect of polymeric carrier

Fig. 1(a) shows the DSC and TGA results for a chemically stabilized cristobalite precursor obtained from PVA solution process. Thermal analysis revealed a two step weight loss with corresponding exothermic curves. The first weight loss was observed up to 200°C. This was associated with decomposition of NO_x compounds, from nitrate salt, and the pyrolysis of polymeric carrier.[20,29] The second major weight loss in TGA occurred between 200°C and 400°C with a corresponding exotherm in the DSC curve. The weight loss was caused by the burnout of the pyrolized organics.[29] In case of the precursor prepared using 85 wt% Pechini resin, the major weight loss, corresponding to two exothermic peaks around 400°C, occurred between 300°C and 500°C, as shown in Fig. 1(b). Further weight loss at higher temperatures was due to the removal of residual carbon. In contrast to the precursor from PVA solution method, NO_x compounds were decomposed during the heating and stirring process. A small exothermic peak, which is associated with crystallization, was detected at around 1050°C in both cases.

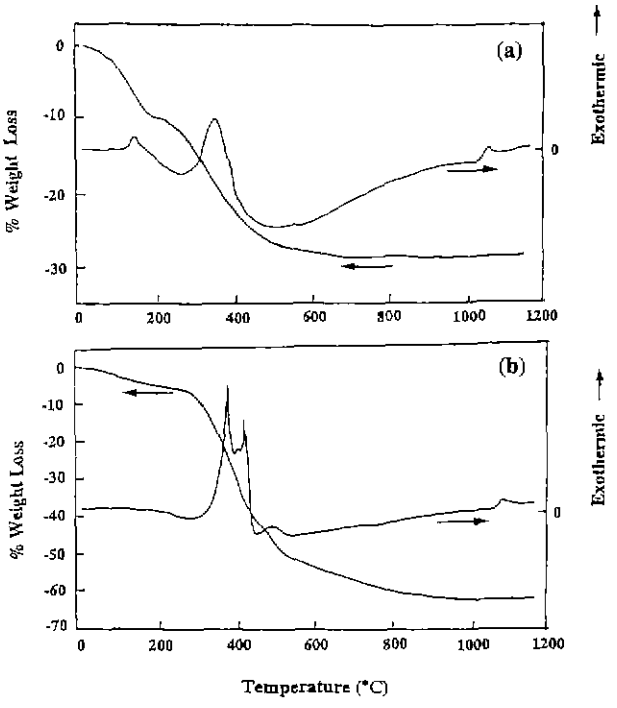

Fig. 1. Simultaneous DSC/TGA analysis of the chemically stabilized β-cristobalite precursors derived from (a) PVA solution and (b) Pechini resin. The composition of the precursors is CaO $2Al_2O_3 \cdot 80SiO_2$.

Fig. 2 shows SEM photographs of both pre and post attrition-milled calcined powders. In case of the calcined powder derived from PVA solution process (Fig. 2(a)), particle size distribution was narrower, and average particle size was smaller than those of the calcined powder prepared by Pechini resin method. The calcined powder showed an elliptical morphology and agglomeration (Fig. 2(a)). In Pechini resin process, the calcined powder showed broad particle size distribution and irregular shape with sharp corners and edges (Fig. 2(c)). The powder was

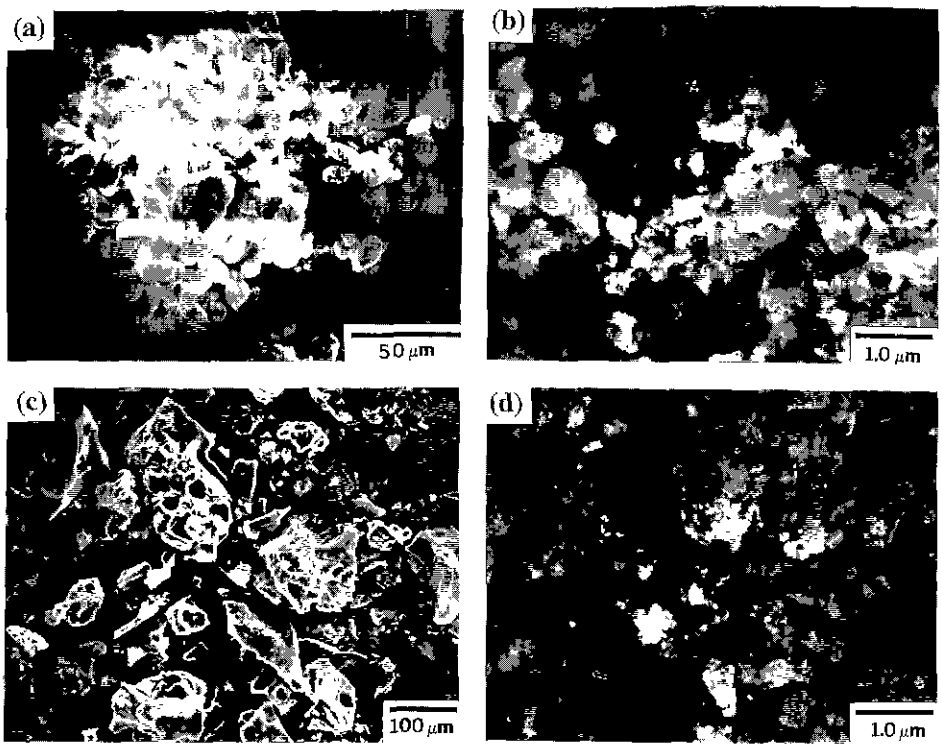

Fig. 2. SEM micrographs showing the effect of the polymeric carriers on the powder morphology (composition of the powders: CaO $2Al_2O_3 \cdot 80SiO_2$). (a) and (b) show the calcined and attrition-milled powders derived from PVA solution, and (c) and (d) show the calcined and attrition-milled powders derived from Pechini resin, respectively.

more porous than the powder derived from PVA solution process. The attrition-milled powder derived from PVA solution process showed comparatively narrower particle size distribution, and had an average particle size of about 0.3 μm (Fig. 2(b)). The BET specific surface area of the calcined and attrition-milled powder derived from PVA solution process were 30 m^2/g and 72 m^2/g, respectively. The attriton-milled powder derived from Pechini resin process had a high specific surface area of 103 m^2/g with a broad particle size distribution (the specific surface area of calcined powder: 24 m^2/g) (Fig. 2(d)). The high specific surface area of the calcined powders prepared by the solution-polymerization route, in spite of larger average particle size than that of the attrition-milled powder, implies that the calcined powder was quite porous and soft.

Fig. 3 shows development of crystalline phases from the precursors at various heating temperatures. An amorphous phase was observed at 1000°C in both cases. Above 1050°C, the β-cristobalite crystalline phase was detected in the powder derived from PVA solution, and β-cristobalite X-ray peaks were developed almost completely at 1200°C. With increasing temperature the amount of α-cristobalite phase increased gradually, while the amount of β-cristobalite decreased. At 1400°C, β-cristobalite remained as a minor phase in the α-cristobalite matrix. In case of the precursor derived from Pechini resin process, the development of crystalline phase was a little delayed in comparison with the case of

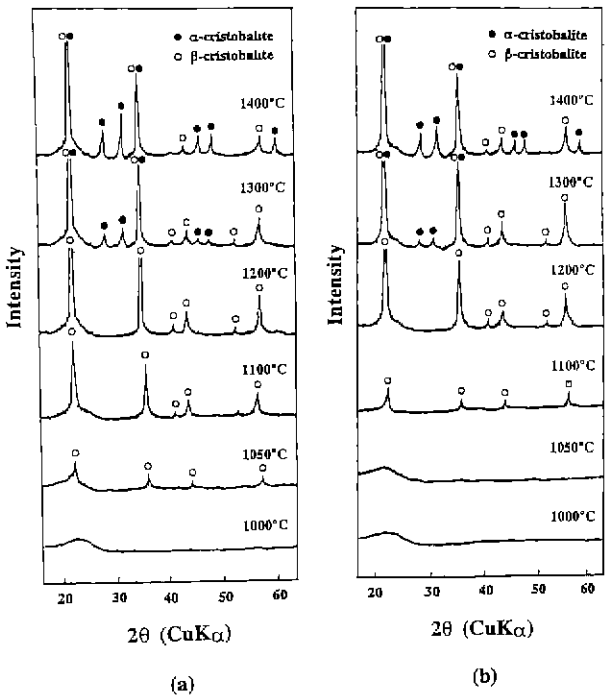

Fig. 3. X-ray diffraction patterns showing the development of crystalline cristobalite from the precursors derived from (a) PVA solution and (b) Pechini resin. The composition of the precursors is $CaO \cdot 2Al_2O_3 \cdot 80SiO_2$.

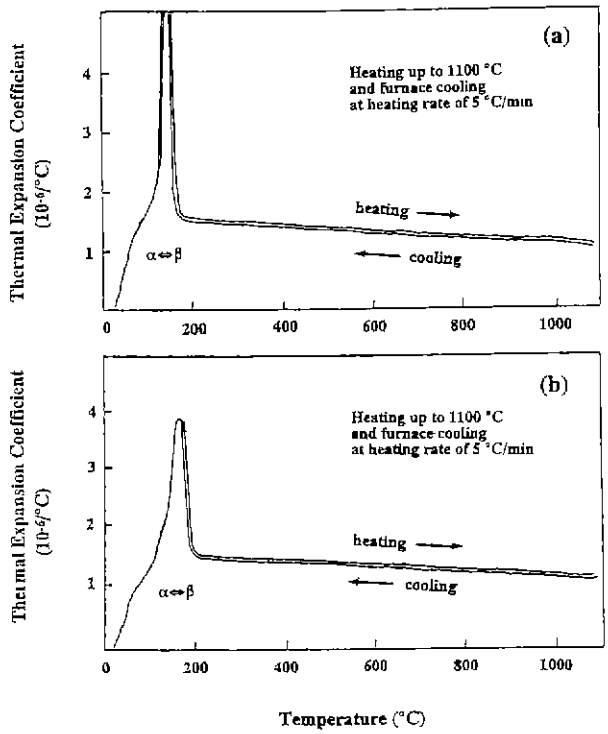

Fig. 4. Dilatometry curves for polycrystalline cristobalite samples derived from (a) PVA solution and (b) Pechini resin. The samples having a $CaO \cdot 2Al_2O_3$ $80SiO_2$ composition were sintered at 1300°C for 1 h.

PVA solution process. Dilatometry curves for the stabilized cristobalites are shown in Fig. 4. The α ⇔ β transformation occurred at 180°C on heating and at 170°C on cooling. Transformation temperature was lower than that of pure cristobalite because of the dopant effect.[3] As the graphs show, the thermal expansion coefficient of β-cristobalite was approximately 1.5×10^{-6}/°C and tended to decrease on heating. A change in thermal expansion coefficient was observed at the α ⇔ β transformation temperature. This change was less for the polycrystalline cristobalite derived from Pechini resin process than the one derived from PVA solution process. The difference in the change of thermal expansion coefficient was attributed to the content of α-cristobalite phase in the polycrystalline cristobalite.

Finally, microstrctures of the sintered and subsequently annealed cristobalite are shown in Fig. 5. In both cases, intergranular cracks were observed. The cracks occurred spontaneously due to thermally-induced phase transformation on cooling. The microstructure was more homogeneous in the case of the sintered cristobalite derived from PVA solution process.

2. *Effect of dopant (stuffing cation) content*

The phases present and porosity for sintered cristobalite at different molar ratios are listed in Table 1. Densification of cristobalite was improved with increasing dopant content at 1100°C. At 1300°C, almost complete densificaton was

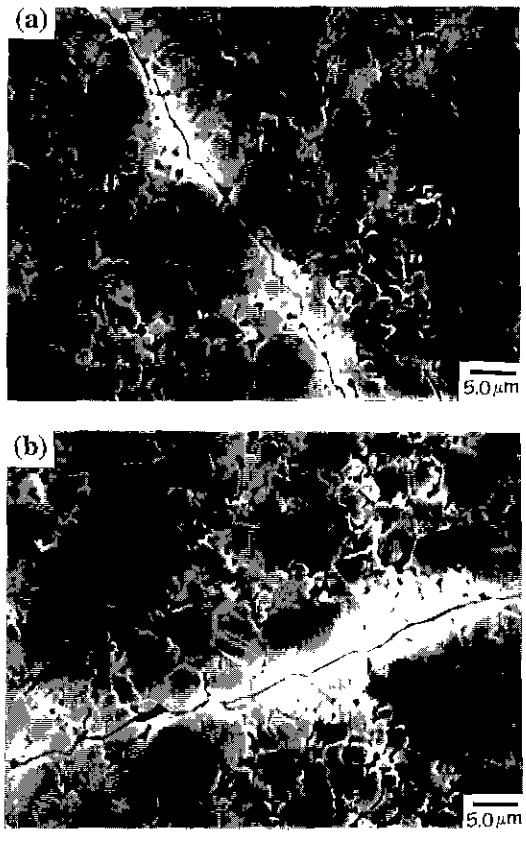

Fig. 5. SEM photographs of polished and etched surfaces of sintered cristobalite specimens derived from (a) PVA solution and (b) Pechini resin. The specimens were sintered at 1300°C for 1 h and annealed for 30 h at 1250°C. The composition of the cristobalite specimens is $CaO \cdot 2Al_2O_3 \cdot 80SiO_2$.

Table 1. Sinterability and Development of Crystalline Phase for Chemically Stabilized β-Cristobalite at Different Dopant Content as a Function of Sintering Temperature

Composition	Sintering temperature (°C)	Porosity (%)	Phases observed by XRD
$CaO \cdot 2Al_2O_3$ $40SiO_2$	1100	0.9	β-cristobalite (amorphous)*
	1300	0.5	β-cristobalite (amorphous)*
CaO $2Al_2O_3$ $60SiO_2$	1100	2.5	β-cristobalite (amorphous)*
	1300	0.8	β-cristobalite (α-cristobalite)
CaO $2Al_2O_3 \cdot 80SiO_2$	1100	5.3	β-cristobalite amorphous
	1300	1.6	β-cristobalite (α-cristobalite)

( ): indicates much smaller amount relative to other phases present.
*amorphous phase ovserved by TEM.

achieved for all specimens and the difference in porosity was reduced. In $CaO \cdot 2Al_2O_3 \cdot 40SiO_2$ composition, amorphous phase was detected in the densified sample. In contrast, the densified sample having a composition of CaO $2Al_2O_3$ $80SiO_2$ showed a small amount of α-cristobalite phase in the β-cristobalite matrix. No amorphous phase was detected in this case. The amorphous phases detected in all compositions at 1100°C were due to incomplete crystallization of amorphous-type β-cristobalite

Table 2. Results of the Relation Between Phase Transformation and Grain Size as a Function of Annealing Time at Different Dopant Content

Composition	Annealing time at 1250° (h)	Ratio of α/β XRD peak intensity (%)	Average grain size (μm)	Thermally induced crack
$CaO \cdot 2Al_2O_3 \cdot 40SiO_2$	0	≈0	1.5	No
	10	18	3.0	No
	30	43	4.5	Yes
$CaO \cdot 2Al_2O_3 \cdot 60SiO_2$	0	4	1.6	No
	10	29	3.4	No
	30	49	5.1	Yes
CaO $2Al_2O_3$ $80SiO_2$	0	12	2.0	No
	10	48	4.4	Yes
	30	68	5.9	Yes

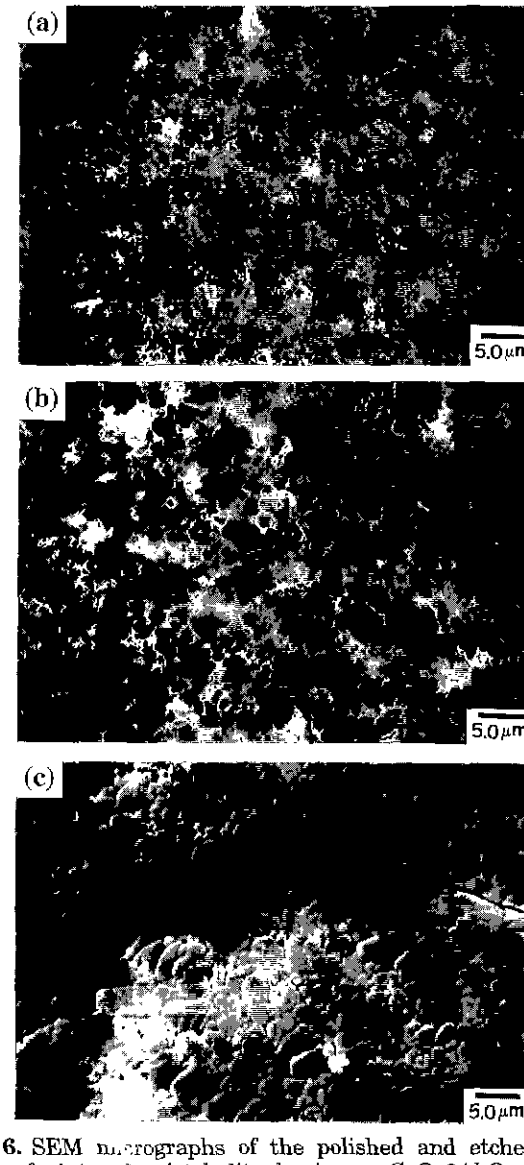

Fig. 6. SEM micrographs of the polished and etched surfaces of sintered cristobalite having a $CaO \cdot 2Al_2O_3 \cdot 40SiO_2$ composition at various annealing times of (a) 0 h, (b) 10 h, and (c) 30 h.

The induced phase transformation behavior of β-cristobalite depended on the grain size, which was affected by annealing time and amount of dopant content. The results of the relation between phase transformation and grain size as a function of annealing time at different compositions are summarized in Table 2. Typically, average grain size increased with increasing annealing time. The content of the thermally-induce transformed a phase also increased with increasing average grain size. Thermally-induced cracks, which occurred spontaneously by critical size effect[26,27] on cooling, were observed in the specimens having an average grain size of about 4.0 μm and above. Microstructures of the sintered cristobalite at different annealing times are shown in Figs. 6 and 7. In case of the densified cristobalite having a high dopant content, the microstructure after sintering was denser, and the average grain size was smaller than the cristobalite containing small amount dopant (Figs. 6(a) and 7(a)). In particular, the rate of grain growth during the annealing time was different in each case. A faster grain growth was observed in the cristobalite having a lesser dopant content. Thermally-induced cracks were observed at the sintered cristobalite, which had an average grain size of 4.0 μm or above, as mensioned in Table 2. The sample having an average grain size of 3.4 μm and $CaO \cdot 2Al_2O_3$ $60SiO_2$ composition did not have any continuous intragranular cracks in the internal texture even though some thermally-induce transformed a-cristobalite was detected (Table 2).

The transformation of β to α-cristobalite was also susceptible to the influence of shear stress. Shear stress-induced β→α-cristobalite conversion for annealed and ground specimens at various annealing times and different dopant contents are compared with unground specimens in Fig. 8. The amount of transformed α phase by shear stress increased with increasing annealing time. In case of the high dopant content, the increase in amount of shear-induce transformed α phase in the ground specimens was slightly higher than the unground specimens. About 5 vol% α-cristobalite was increased by the shear-induced transformation at annealing for 30 h. In comparison, the specimens containing low dopant content were more sensitive to shear stress. An increase of about 13 vol% α-cristobalite was calculated above 10 h of

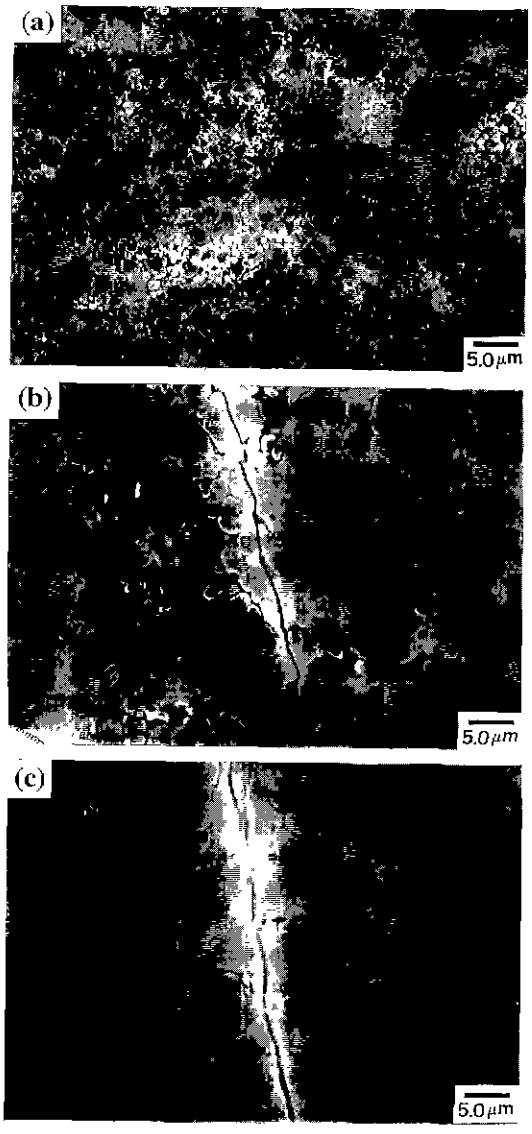

Fig. 7. SEM micrographs of the polished and etched surfaces of sintered cristobalite having a CaO $2Al_2O_3$ $80SiO_2$ composition at various annealing times of (a) 0 h, (b) 10 h, and (c) 30 h.

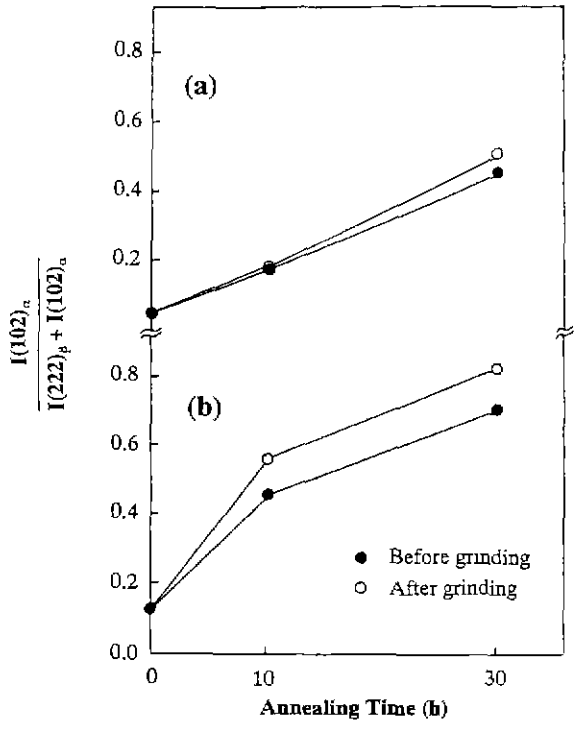

Fig. 8. Grinding effect on the ratio of α/β XRD peak intensity of sintered cristobalite having a composition of (a) $CaO \cdot 2Al_2O_3 \cdot 40SiO_2$ and (b) $CaO \cdot 2Al_2O_3$ $80SiO_2$ at various annealing times.

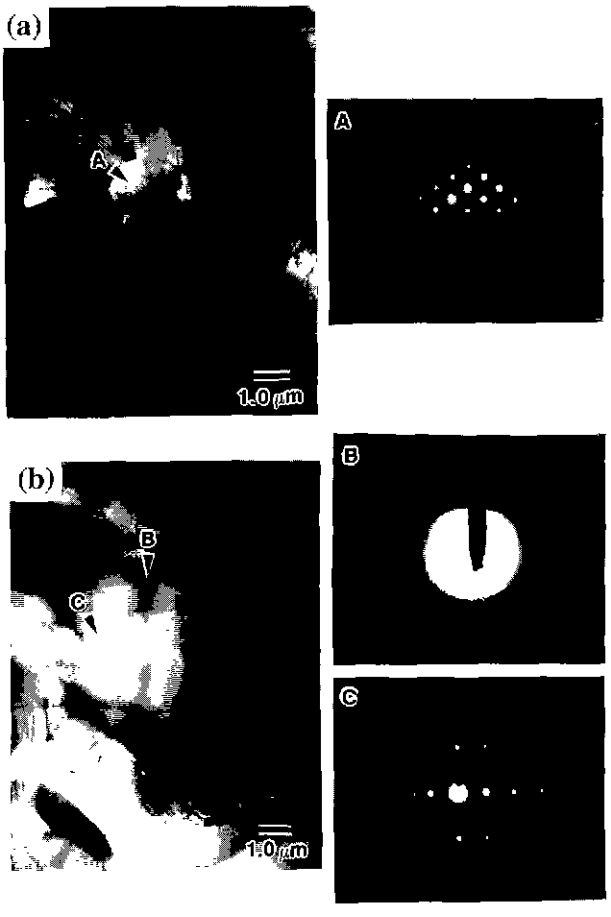

Fig. 9. Bright-field TEM micrographs and corresponding SAD patterns of the sintered cristobalite specimens of (a) $[1\bar{1}0]_c$ zone axis diffraction pattern from unannealed β-cristobalite and (b) $[021]_t$ zone axis diffraction pattern from induce-transformed α-cristobalite after annealing for 30 h. Arrow B shows the presence of a intergranular glassy phase. The composition of the specimens is $CaO \cdot 2Al_2O_3 \cdot 40SiO_2$.

annealing time.

Transmission electron microscopy studies confirmed the critical size effect on the phase transformation of cristobalite. Fig. 9 shows the TEM bright-field image of a and β-cristobalite grains and corresponding SAD patterns of the sintered cristobalite having a composition of $CaO \cdot 2Al_2O_3 \cdot 40SiO_2$. A cubic β-cristobalite pattern was revealed in the unannealed specimen.[23] The specimen annealed for 30 h showed a tetragonal α-cristobalite pattern for the grain with a size of 4 μm and above. Intergranular glassy phase (arrow B) was also found.

IV. Discussion

The calcined powders showed totally different morphologies with different polymeric carriers. A narrower particle size distribution and smaller average particle size were observed in the calcined powder derived from PVA solution process. Moreover, the precusor prepared by PVA solution process showed faster organic burnout behavior and development of crystallization than the precursor derived from Pechini resin process. These results indicate that chelation of the metal ions by the carboxylic end groups, as in the Pechini resin case, is not the only route to obtain chemically stable precursor. The results also showed that a fine and homogeneous silicate powder can be produced by polymerization mechanism via stearic entrapment of the metal ions by hydroxyl functional groups. The large chain molecules of PVA acted as a more effective polymeric carrier in the solution-polymerization technique in spite of the small amount of polymer in the 5 wt% PVA solution.

Submicron powder, which have high specific surface area, could be obtained by attrition-milling for just 1 h. It was attributed to the soft and porous nature of the calcined powder.

Content of oxide dopants, CaO, Al_2O_3, affected the sinterability and grain growth of polycrystalline cristobalite as well as the stabilization of cubic silica. Excess dopant content enhanced densification but it remained as a residual intergranular glassy phase in the cristobalite matrix. The glassy phase decreased the critical size effect on the shear-induced phase transformation. However, thermally-induced transformation behavior was independent of the glassy phase. At similar average grain size, the amount of thermally-transformed α-cristobalite was almost identical, as shown in Table 2. The spontaneous thermally-induced cracks occurred at the average grain size of 4.0 μm or above by critical size effect. In order to use the chemically stabilized β-cristobalite for the transformation weakening mechanism, more extensive shear stress induced transformation is desirable. For that, the chemically stabilized β-cristobalite containing lesser amount of dopant ($CaO \cdot 2Al_2O_3 \cdot 80SiO_2$), which is more sensitive to shear stress, is required.

V. Conclusions

A solution-polymerization route has been employed for the preparation of chemically stabilized β-cristobalite powder. The characteristics of powder and its sintered sample were affected by the type of polymeric carrier and amount of dopant. PVA solution process was more effective to prepare the β-cristobalite powder having a fine and narrow particle size distribution than did Pechini resin precess.

Intergranular glassy phase in the sintered cristobalite, formed by excess dopant content, lowered the response to induced phase transformation by shear stress. A critical grain size for the $\beta \rightarrow \alpha$ transformation was about 4.0 μm and 13 vol% shear induce transformed α-cristobalite was observed at around the critical grain size, in the $CaO \cdot 2Al_2O_3 \cdot 80SiO_2$ composition.

References

1. A. F. Wright and A. J. Leadbetter, "The Structures of

the β-cristobalite Phase of SiO_2 and $AlPO_4$," *Philos. Mag.*, **31**, 1391-401 (1975).
2. D. A. Peacor, "High-Temperature Single-Crystal Study of the Cristobalite Inversion," *Z. Kristallogr.*, **138**, 274-98 (1973).
3. V. G. Hill and R. Roy, "Silica Structure Studies: V, The Variable Inversion in Cristobalite," *J. Am. Ceram. Soc.*, **41**[12], 532-37 (1958).
4. W. M. Kriven, "Possible Alternative Transformation Toughened to Zirconia: Crystallographic Aspects," *J. Am. Ceram. Soc.*, **71**[12], 1022-30 (1988).
5. W. M. Kriven, "Displacive Phase Transformation and Their Applications in Structural Ceramics," *J. de Physique IV, Colloque* **C8**, 101-110 (1995).
6. W. M. Kriven and S. J. Lee, "Phase Transformation Weakening Behavior of Chemically Stabilized β-cristobalite, Part II. Mullite/Cordierite Laminates with a β-cristobalite Interphase," *J. Am. Ceram. Soc.*, (1997), submitted.
7. S. C. Mirek, "Phase Transformation Weakening in Fibrous Ceramic Composites; An Investigation of the Enstatite ($MgSiO_3$)/Titania (TiO_2) System," M.S Thesis, Univ. Illinois at Urbana-Champaign, 1995.
8. W. J. Clegg, "The Fabrication and Failure of Laminar Ceramic Composites," *Acta Metall.*, **40**[11], 3085-93 (1992).
9. C. N. Fenner, "Stability Relations of the Silica Minerals," *Am. J. Sci. [4th Series]*, **36**(214), 331-84 (1913).
10. W. Eitel, "Structural Anomalies in Tridymite and Cristobalite," *Am. Ceram. Soc. Bull.*, **36**[4], 142-48 (1957).
11. M. J. Buerger, "Stuffed Derivatives of the Silica Structures," *Am. Mineral.*, **39**[7-8], 600-14 (1954).
12. A. J. Perrotta, D. K. Grubbs, E. S. Martin and N. R. Dando, "Chemical Stabilization of β-cristobalite." *J. Am. Ceram. Soc.*, **72**[3], 441-47 (1989).
13. E. S. Thomas, J. G. Thompson and R. L. Withers, "Further Investigation of the Stabilization of β-cristobalite." *J. Am. Ceram. Soc.*, **77**[1], 49-56 (1994).
14. J. B. Parise, D. J. Weidner, J. D. Jorgensen and M. A. Saltzberg, "Pressure-Induced Phase Transition and Pressure Dependence of Crystal Structure in Low (α) and Ca/Al-Doped Cristobalite." *J. Appl. Phys.*, **75**[3], 1361-66 (1994).
15. M. A. Gulgun and W. M. Kriven, "A Simple Solution-Polymerization Route for Oxide Powder Synthesis;" pp. 57-66 in Ceramic Transactions, Vol. 62, *Science, Technology, and Commercialization of Powder Synthesis and Shape Forming Processes*. Edited by J. J. Kingsley, C. H. Schilling, and J. H Adair, American Ceramic Society, Westerville, OH, 1996
16. M. A. Gulgun, M. H. Nguyen and W. M. Kriven, "Polymeric Organic-Inorganic Synthesis of Mixed Oxides," *J. Am. Ceram. Soc* , (1996), submitted.
17. S. J. Lee and W. M. Kriven, "Nano-size Amorphous Cordierite Powder Prepared by a Solution-Polymerization Route," *J. Am. Ceram. Soc.*, (1997), submitted.
18. M. H. Nguyen and W. M. Kriven, "Chemical Synthesis of Dysprosium Titanate via Stearic Entrapment," *J. Am. Ceram. Soc.*, (1997), submitted.
19. M. Pechini, "Method of Preparing Lead and Alkaline-Earth Titanates and Niobates and Coating Method Using the Same to Form a Capacitor," U.S. Pat. No. 3 330 697, July 11, 1967.
20. D. Budd and D. A. Payne, "Preparation of Strontium Titanate Ceramics and Internal Boundary Layer Capacitors by the Pechini Method," *Mater. Res. Soc. Symp. Proc.*, **32**, 239 (1984).
21. L. W. Tai and P. A. Lessing, "Modified Resin-Intermediate Processing of Perovskite Powder: Part I. Optimization of Polymeric Precursors," *J. Mater. Res.*, **7**[2], 502-510 (1992).
22. L. W. Tai and P. A. Lessing, "Modified Resin-Intermediate Processing of Perovskite Powder: Part II. Processing for Fine, Nonagglomerated Sr-Doped Lanthanum Chromite Powders," *J. Mater. Res.*, **7**[2], 511-519 (1992).
23. P. A. Lessing, "Mixed-Cation Oxide Powder via Polymeric Precursors," *Am. Ceram. Soc. Bull.*, **68**[5], 1002-1007 (1989).
24. K. Toyoshima, "General Properties of Polyvinyl Alcohol in Relation to its Applications"; pp. 22-42 in Polyvinyl Alcohol Properties and Applications. Edited by C. A. Finch John Wiley &Sons, New York, 1973.
25. R. T. DeHoff and F. N. Rhines, *Quantitative Microscopy*. McGraw-Hill, New York, 1968.
26. W. M. Kriven, C. J. Chan and E. A. Barinek, "The Particle-Size Effect of Dicalcium Silicate in a Calcium Zirconate Matrix"; pp. 145-55 in Advances in Ceramics, Vol. 24, *Science and Technology of Zirconia III*. Edited by S. Somiya, N. Yamamoto, and H. Hanagida. American Ceramic Society, Westerville, OH, 1988.
27. C. M. Huang, D. H. Kuo, Y. J. Kim and W. M. Kriven, "Phase Stability of Chemically Derived Enstatite ($MgSiO_3$) Powders." *J. Am. Ceram. Soc.*, **77**[10], 2625-31 (1994).
28. R. L. Withers, J. G. Thompson and T. R. Welberry, "The Structure and Microstructure of α-cristobalite and Its Relationship to β-cristobalite," *Phys. Chem. Minerals*, **16**, 517-523 (1989).
29. B. C. Mutsuddy, "Oxidation Removal of Organic Binders from Injection-molded Ceramics." in Non-oxide Technical and Engineering Ceramics, Elsevior Applied Sci., New York. pp. 397-408, (1986).